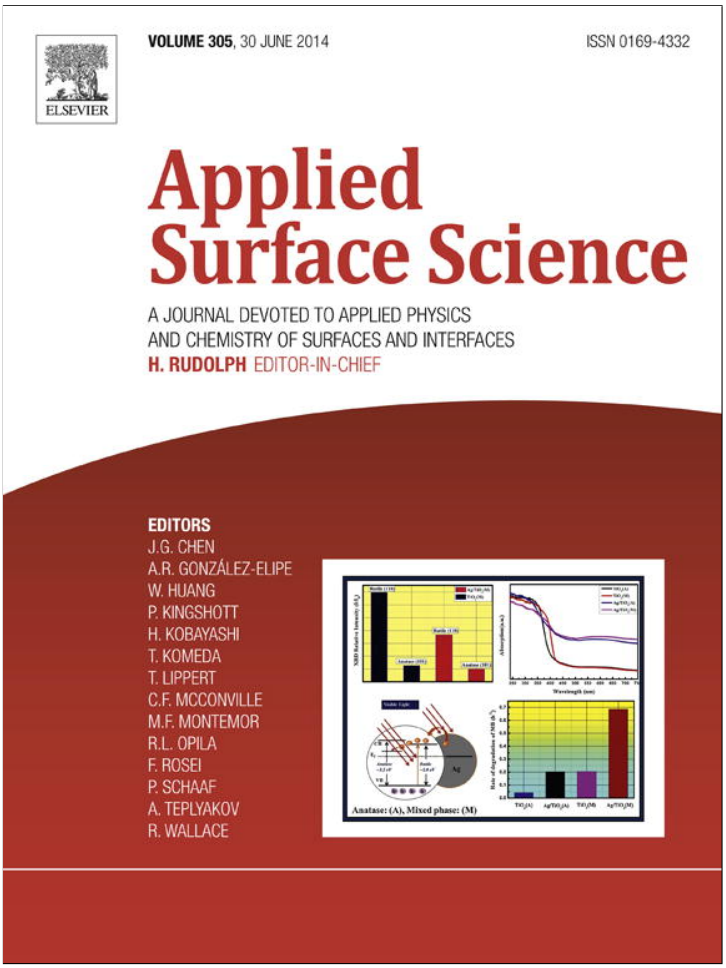

Applied Surface Science 305 (2014) 67–76

Contents lists available at ScienceDirect

Applied Surface Science

journal homepage: www.elsevier.com/locate/apsusc

Dielectric properties and thermal destruction of poly(dimethylsiloxane)/Fe_2O_3/SiO_2 nanocomposites

M.V. Galaburda[a,*], P. Klonos[b], V.M. Gun'ko[a], V.M. Bogatyrov[a], M.V. Borysenko[a], P. Pissis[b]

[a] Chuiko Institute of Surface Chemistry, 17 General Naumov Street, 03164 Kiev, Ukraine
[b] Department of Physics, National Technical University of Athens, 15780 Athens, Greece

ARTICLE INFO

Article history:
Received 26 November 2013
Received in revised form 26 February 2014
Accepted 26 February 2014
Available online 12 March 2014

Keywords:
Nanosilica
Fe_2O_3/SiO_2 nanocomposite
Poly(dimethilsiloxane)
SiO_2/PDMS
Thermogravimetry
Differential scanning calorimetry
Thermally stimulated depolarization current
Dielectric relaxation spectroscopy
Hydrophobicity

ABSTRACT

Thermally stimulated chemical transformation of poly(dimethilsiloxane) (PDMS) adsorbed onto highly disperse Fe_2O_3/SiO_2 was studied using FTIR, thermogravimetry and differential thermal analysis. The influence of active surface sites on this transformation was investigated since iron oxide affects the degradation of PDMS. It was shown that PDMS provides stable (in the 100–500 °C range) hydrophobic properties to SiO_2/PDMS depending on PDMS concentration. Differential scanning calorimetry, thermally stimulated depolarization currents and dielectric relaxation spectroscopy techniques were employed to investigate the effects of iron oxide on thermal transitions (in particular glass transition), segmental dynamics and interfacial interactions in PDMS/oxides nanocomposites.

1. Introduction

Polymer nanocomposites (usually at low filler content) have attracted attention due to their exceptional mechanical and other properties compared to those of conventional micro and macroscale composites. Incorporation of different inorganic components into siloxane-based structures has been carried out in order to improve the mechanical, thermal, electrical and optical properties and dimensional stability of the polymer matrix or to obtain new properties derived from the hybrid nature of the materials [1,2]. Aerogels and fumed silica composed of nanoparticles are the most preferred fillers for silicones. Other components such as ferric oxide, titanium dioxide or organometallic compounds can be added as heat stabilizers or pigments [3]. Addition of nanostructured materials such as TiO_2 or ZrO_2 to improve resistance to thermodegradation or Al_2O_3 to improve thermal conductivity, abrasive and flame resistance [4] can widen the applications of PDMS based nanocomposites. The effects of in-situ synthesized titania nanoparticles on thermal transitions, segmental dynamics and interfacial interactions in poly(dimethylsiloxane)/titania nanocomposites were studied in detail [5].

It is known that the properties of nanocomposites can be improved due to modification of a filler structure that results in changes in the polymer dynamics due to changes in interactions with filler particles. A great surface-to-volume ratio for nanoparticles leads to dominance of a polymer fraction located close to interfaces. Therefore, the composite properties strongly depend on the characteristics of this fraction. The polymer dynamics and the glass transition in nanocomposites are more complex than in neat polymers [5]. Therefore, the mechanisms of the interfacial phenomena in composites need additional and detailed investigation, in particular with respect to the effect of filler structure and modification. It was shown [6] that increase of the glass transition temperature T_g in polymer nanocomposites is due to the nanoparticles, that restrict the mobility of the entire volume of the polymer. Reduction of T_g was established in the case of weak interactions between a filler and a polymer [7]. In another work, addition of nanoparticles was found to cause insignificant changes in the glass transition of the polymer presumably because the effects causing an increase or decrease in the polymer mobility are present simultaneously and are effectively cancelled out [8]. The molecular dynamics

* Corresponding author. Tel.: +380977188971.
E-mail address: mashagayeva@yandex.ru (M.V. Galaburda).

http://dx.doi.org/10.1016/j.apsusc.2014.02.162
0169-4332/

of a series of poly(dimethylsiloxane) filled with silica nanoparticles synthesized in-situ were investigated [9] using differential scanning calorimetry (DSC), thermally stimulated depolarization current (TSDC) and broadband dielectric relaxation spectroscopy (DRS) and it was shown that polymer mobility is reduced in an interfacial layer 2–3 nm thick around the nanoparticles.

Gee et al. [10] studied the effect of adsorbed water on the interfacial structure and dynamics in silica–polydimethylsiloxane composites using molecular dynamics (MD). They concluded that polymer chains mobility significantly decreased with decreasing hydration level. The reduced mobility of the PDMS chains in the interfacial domain reduced the overall, bulk, motional properties of the polymer, thus causing an effective "stiffening" of the polymer matrix.

Considering polymer/silica interactions using a variety of matrices studied by dynamical mechanical analysis (DMA) and DRS [11] results were interpreted using a three-layer model with strongly bound (which does not participate in the glass transition), loosely bound (responsible for a second glass transition) and quasi-bulk (unaffected by the particles) fractions of the polymer. On the other hand, DMA [12] and neutron scattering results [13] in polymer/silica nanocomposites were explained in terms of a two-layer model: a single interfacial layer with reduced dynamics and quasi-bulk polymer. The aim of this paper was to elucidate the influence of silica modification by Fe_2O_3 on the interfacial behavior of PDMS.

2. Materials and methods

2.1. Materials

Fumed silica (pilot plant of the Chuiko Institute of Surface Chemistry, Kalush, Ukraine, $S = 290\ m^2/g$) was used as a matrix. Fe(III) acetylacetonate ($Fe(acac)_3$, Aldrich, >98% $Fe(acac)_3$) was used as a precursor of synthesized iron oxide nanoparticles on the silica surface.

Fe_2O_3/SiO_2 samples were synthesized by impregnation of the silica powder (pre-heated at 120 °C for 2 h) by $Fe(acac)_3$ dissolved in isopropanol at 3 wt% with respect to dry silica, with subsequent drying (82 °C) and oxidation (500–600 °C) in air. The concentration of iron oxide in the sample was 4 wt%.

Then PDMS ("Kremniypolimer", Zaporozhye, Ukraine, molecular weight $W_m \approx 7960$, degree of polymerization 105) was adsorbed onto the initial silica and Fe_2O_3/SiO_2 samples in the amount of 10, 20, 30, 40, and 80 wt%. Before the adsorption, oxide samples were dried at 110 °C for 1 h, and then a solution of PDMS in hexane (oxide + PDMS ~ 11 wt%) was added and stirred. The suspension was dried at room temperature for 24 h and then at 80 °C for 3 h.

2.2. Diffuse reflectance infrared Fourier transform spectroscopy (DRIFT)

The DRIFT spectra of dried powdered samples (grinded with KBr at the mass ratio 1:9) were recorded over the 4000–400 cm^{-1} range in a diffuse reflectance mode using a ThermoNicolet Nexus FTIR spectrometer spectrometer. The reflectance data were converted to absorbance using program "Omnic 6.1".

2.3. Specific surface area

The specific surface area (S_{Ar}) was calculated using adsorption of argon (from an Ar/He mixture) at 77.4 K with a LKhM-72 (Russia) chromatograph and Silochrome-80 as a reference material.

2.4. Thermogravimetry (TG)

Thermal analysis of PDMS adsorbed on oxide samples (weight ~200 mg) was carried out in air at 288–1273 K using a Derivatograph Q-1500D (Paulik, Paulik & Erdey, MOM, Budapest) with TG-DTA (differential thermal analysis) at a heating rate of 10 K/min.

2.5. Differential scanning calorimetry (DSC)

Thermal transitions of the materials were investigated in helium atmosphere in the −175–0 °C range using a TA Q200 series DSC instrument, calibrated with Indium (for temperature and enthalpy) and sapphires (for heat capacity). Samples of ~8 mg in mass, taken from the produced powders, were closed in standard aluminum pans. Cooling and heating rates were 10 °C/min. It should be noted that PDMS crystals are melted at room temperature, so the first heating scan for erasing thermal history [14] was not necessary here.

Using the crystallization, cold crystallization and melting enthalpies, ΔH_c, ΔH_{cc} and ΔH_m, respectively, as recorded through DSC and also normalized to the same polymer content X_{PDMS} for each sample, the degrees of crystallinity $X_{c,cryst}$ and $X_{c,melt}$ were calculated according to Eqs. (1) and (2), in which $\Delta H_{100\%}$ is the enthalpy of PDMS fusion, taken as 37.43 J/g [15]. We also normalized the heat capacity change at glass transition as recorded from DSC, $\Delta C_{p,DSC}$, to the amorphous polymer fraction according to Eq. (3).

$$X_{c,\mathrm{cryst}} = \frac{\Delta H_c}{(X_{\mathrm{PDMS}} \times \Delta H_{100\%})} \quad (1)$$

$$X_{c,\mathrm{melt}} = \frac{(\Delta H_m - \Delta H_{cc})}{(X_{\mathrm{PDMS}} \times \Delta H_{100\%})} \quad (2)$$

$$\Delta C_{p,\mathrm{norm}} = \frac{\Delta C_{p,\mathrm{DSC}}}{(X_{\mathrm{PDMS}}\,(1 - X_c))} \quad (3)$$

2.6. Thermally stimulated depolarization current (TSDC)

Thermally stimulated depolarization current is a special dielectric technique working in the temperature domain and characterized by high sensitivity and high resolving power. The latter is due to the low equivalent frequency of the technique (10^{-4}–10^{-2} Hz) [16]. A sample (compressed to form a cylindrical pellet of 12 mm in diameter and 1–2 mm in thickness) was inserted between the brass plates of a capacitor, placed in a Novocontrol TSDC sample cell and polarized by an electrostatic field E_p (~100 V/mm) with a home-made voltage source at polarization temperature $T_p = 20$ °C for $t_p = 5$ min. With the field still applied, the sample was cooled to −150 °C (cooling rate 10 °C/min, under nitrogen flow), sufficiently low to prevent depolarization by thermal energy, then short-circuited and reheated up to 50 °C at a constant heating rate $b = 3$ °C/min. Temperature control was achieved by means of a Novocontrol Quatro cryosystem. A discharge current was generated during heating and measured as a function of temperature with a sensitive programmable Keithley 617 electrometer.

2.7. Dielectric relaxation spectroscopy (DRS)

For dielectric relaxation spectroscopy [17] measurements, the sample (the same as used for TSDC measurements) was placed between the plates of a capacitor and an alternate voltage was applied in a Novocontrol sample cell. The complex dielectric permittivity, $\varepsilon^* = \varepsilon' - i\varepsilon''$, was recorded isothermally as a function of frequency in the range from 10^{-1} to 10^6 Hz at temperature from −150 °C to 60 °C (in nitrogen atmosphere) in steps of 2.5, 5 and 10 °C (depending on the process to be studied) using a Novocontrol

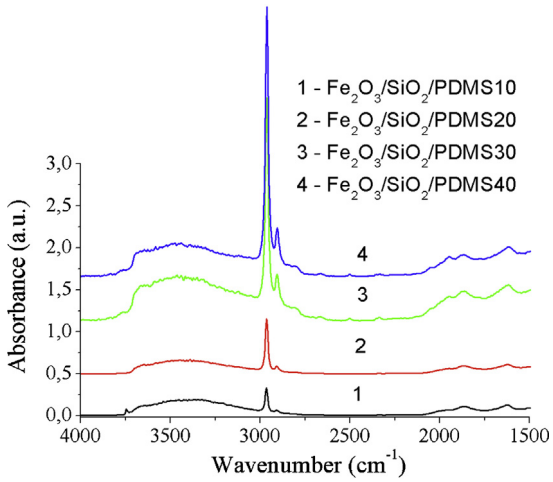

Fig. 1. DRIFT spectra of Fe_2O_3/SiO_2/PDMS samples mixed with KBr (1:9).

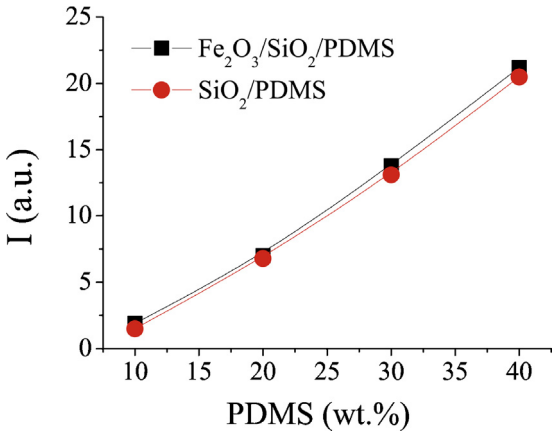

Fig. 2. Integral intensity of the bands of CH stretching vibrations of CH_3 groups vs. the PDMS content.

Alpha analyzer. The temperature was controlled better than ±0.5 °C with a Novocontrol Quatro cryosystem.

2.8. Hydrophobicity

The hydrophobicity of the samples was measured as a contact angle value for water drops placed onto a sample surface using a sessile drop method with a USB digital microscope (Sigeta, China, magnification ratio 20× to 200×). A drop of distilled water was applied to a pressed pellet with an oxide/PDMS sample previously heated at 80–700 °C for 0.5 h (this treatment results in temperature-dependent degradation of the PDMS layer differently affected by silica and Fe_2O_3/SiO_2 surfaces). Measurements were carried out in air at room temperature (18 ± 0.5 °C). The calculations were made using data described elsewhere [18].

3. Results and discussion

3.1. Characteristics of oxide and PDMS/oxide systems

The FTIR spectra (Fig. 1) show that PDMS molecules interact with the silica surface since the intensity of the band of free silanols at 3750 cm^{-1} decreases with increasing polymer fraction due to the hydrogen bonding to PDMS. The content of adsorbed PDMS was controlled by changes in the C–H stretching vibrations of the CH_3 groups in the 2930–3110 cm^{-1} range (using the Omnic 6.1 program) (Fig. 2). These values were normalized to the intensity of the band at 1865 cm^{-1}. The presence of Fe_2O_3 does not affect on the FTIR spectra of adsorbed PMPS. The spectral patterns depend on the amount of adsorbed polymer. The character of changes of the I_{C-H} value for these two series is the same and has a linear dependence on PDMS content (Fig. 2). That indicates equal content of the polymer on the surface of the samples.

It is known [19] that only a portion of the segments of adsorbed PDMS molecules can interact with a surface with formation of hydrogen bonds ≡MO–H···O($Si(CH_3)_2$–)$_2$ (where M = Si or Fe). Notice that the surface of Fe_2O_3 has different number of hydroxyl groups on the surface (4–5 OH-groups per nm^2 [20]) and they can absorb water, which can promote the reactions of hydrolysis of the polymer, as well as participate in the adsorption of polymer.

3.2. Thermal decomposition of adsorbed PDMS

Thermal decomposition of PDMS on a silica surface was investigated in details [21–23]. Decomposition of PDMS alone can occur in air due to oxidation of methyl groups with the formation of silica (Scheme 1) [24] or due to depolymerization with the formation of hexamethylcyclotrisiloxane (HMETS) (Scheme 2).

$$-OSi(CH_3)_2- + 4\,O_2 \Rightarrow SiO_2 + 2\,CO_2 + 3\,H_2O \qquad \text{(Scheme 1)}$$

$$[\text{-}OSi(CH_3)_2\text{-}]_n \Rightarrow [\text{-}OSi(CH_3)_2\text{-}]_{n-3} + \text{HMETS} \qquad \text{(Scheme 2)}$$

The DTG curves for Fe_2O_3/SiO_2/PDMS samples exhibit three well-defined regions of the mass loss (Fig. 3b). There is correlation between the amount of PDMS (intensity of the peaks) and the temperature of onset of the mass loss (Table 1). The first region is attributed to the removal of physically sorbed water (T = 50–120 °C), while the next two steps are due to oxidation of methyl groups and removal of volatile cyclic siloxanes according to Schemes 1 and 2. According to the content of PDMS in the samples, we calculated the final results of the mass changes in samples during the reactions proceeding according to Schemes 1 and 2. The experimental values of the mass losses of the samples were determined in the interval 120–1000 °C. The calculated and experimental data are presented for comparison in a diagram (Fig. 3). The calculated lower curve (Fig. 3d) corresponds to Scheme 1 and the upper curve represents reaction (5). The experimental data (Fig. 3d) show that the destruction of dimethylsilyl groups in the Fe_2O_3/SiO_2/PDMS precedes mainly according to Scheme 2 with increasing contribution of depolymerization reaction at T > 350 °C. Previously [23] it was shown that oxidation of PDMS/SiO_2 occurs mainly according to reaction (4).

It is evident from the obtained results (Fig. 3) that the thermal decomposition of PDMS on the surfaces of the modified silica begins at lower temperature than in case of initial PDMS/SiO_2. This makes it possible to assert that iron oxide leads to a partial depolymerization of adsorbed PDMS according to Scheme 2, followed by crosslinking of the polymer that leads to loss of flexibility of the chains and the density of PDMS layer increases so final destruction

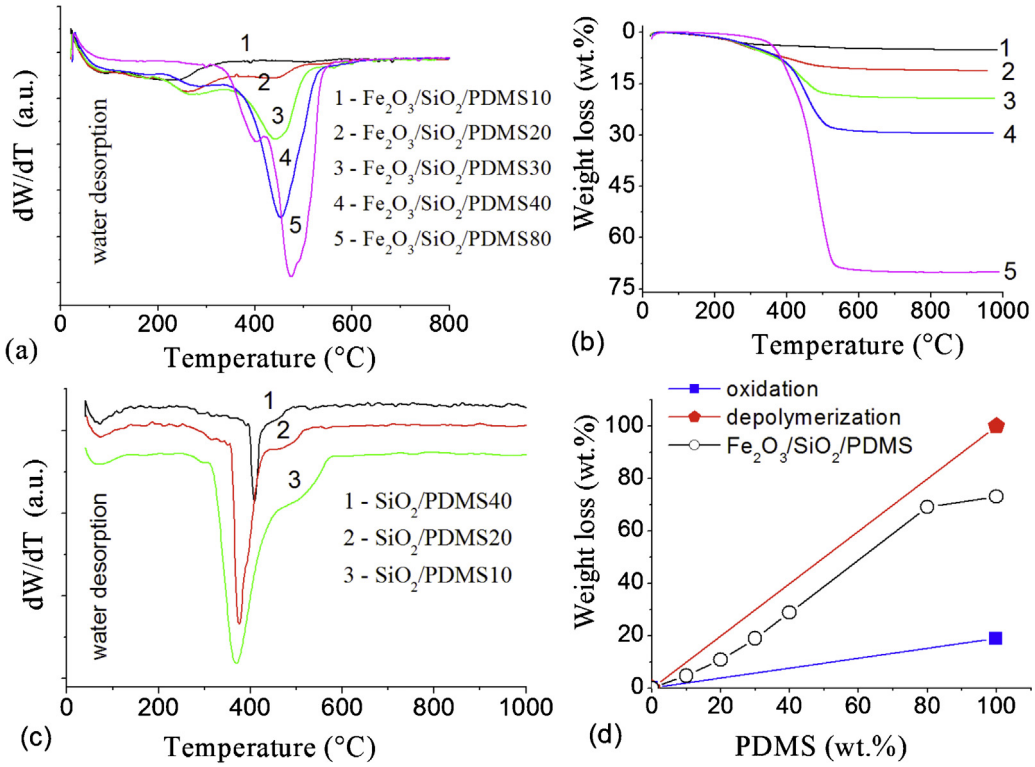

Fig. 3. Differential thermogravimetric (DTG) (a and c) and thermogravimetric (TG) (b) data for Fe_2O_3/SiO_2/PDMS (a and b) and SiO_2/PDMS samples (c); and (d) comparison of experimental and calculated mass loss vs. PDMS content.

occurs at higher temperature. That is illustrated in Fig. 3 by shifting of the DTG peaks toward higher temperatures with increasing of the intensity of the peaks according to the rising of PDMS content. In the case of SiO_2/PDMS, on the contrary, the peaks are shifted toward lower temperature with increasing PDMS content.

The effect of Fe_2O_3 on the thermal destruction of PDMS is well observed in the FTIR spectra of treated samples. The integral intensity of the C–H (I_{C-H} = 3100–2900 cm^{-1}) and O–H (I_{O-H} = 3748 cm^{-1}) stretching vibrations depends on concentration of PDMS (Fig. 4). The SiO_2/PDMS samples are characterized by a decrease in concentration of the methylsilyl groups (I_{C-H}) at $T > 350\,^{\circ}C$ due to the thermal oxidative destruction, whereas for Fe_2O_3/SiO_2/PDMS, thermal destruction begins at lower temperature (~200 °C). The I_{C-H} values regularly decrease at ~200 °C; however, restoring of OH groups is not observed at this temperature. This may be due to destruction of Si–CH_3 groups leading to formation of silica deposits remaining on the surface, and restoring of Si–OH groups can be observed only after complete destruction of organic functionalities.

During the depolymerization, organopolysiloxane can undergo complete transformation into volatile products, which can be chemisorbed on the free silanols to form new arched structures. The oxidation of Si–CH_3 groups is accompanied by the formation of Si–OH groups, which interact with each other to form siloxane bonds Si–O–Si [24]. This can be displayed as a significant increase in the specific surface area (Fig. 5).

The influence of mixed oxides on thermal transformation of the polymer can be estimated by measuring of the hydrophobicity of the samples since silica and iron oxide are hydrophilic but PDMS is hydrophobic. The adsorbed polymer forms a hydrophobic coating on the surface and oxidation of dimethylsilyl groups leads to reconstruction of silanol groups and changing the hydrophobic properties toward hydrophilic ones. Dependence of the contact angle of water drops on calcination temperature of Fe_2O_3/SiO_2/PDMS and SiO_2/PDMS samples shows that the hydrophobic range of Fe_2O_3-contained samples is wider than in case of SiO_2/PDMS (Fig. 6). The maximum contact angle of water drops of SiO_2/PDMS is observed after heating at 300–400 °C and reached 112–116° (20% and 30% wt of polymer). For samples Fe_2O_3/SiO_2/PDMS, maximum angles of 114–116° are observed after heating at 200–350 °C (20–30 wt% of PDMS). Thus, iron oxide shifts the degradation of PDMS toward lower temperatures.

Increasing contact angle of water drops on the surface of the composites containing Fe_2O_3 is due to the formation of a denser PDMS layer under mild temperature conditions. Iron oxide affects the process of PDMS destruction. The chemisorption of the products

Table 1
TG data on mass loss of heated PDMS/oxide samples.

Sample	Mass loss at different temperatures (%)				
	30–120 °C	120–350 °C	350–1000 °C	120–1000 °C	According to Eq. (4)
SiO_2/PDMS40	0.3	3.8	11.9	73	18.9
Fe_2O_3/SiO_2/PDMS10	0.6	3.2	1.5	4.7	1.9
Fe_2O_3/SiO_2/PDMS20	0.5	5.8	5	10.8	3.8
Fe_2O_3/SiO_2/PDMS30	0.5	6.1	12.8	18.9	5.7
Fe_2O_3/SiO_2/PDMS40	0.3	5.6	23.6	29.2	7.6
Fe_2O_3/SiO_2/PDMS80	0.1	3.3	66.8	70.1	15.1

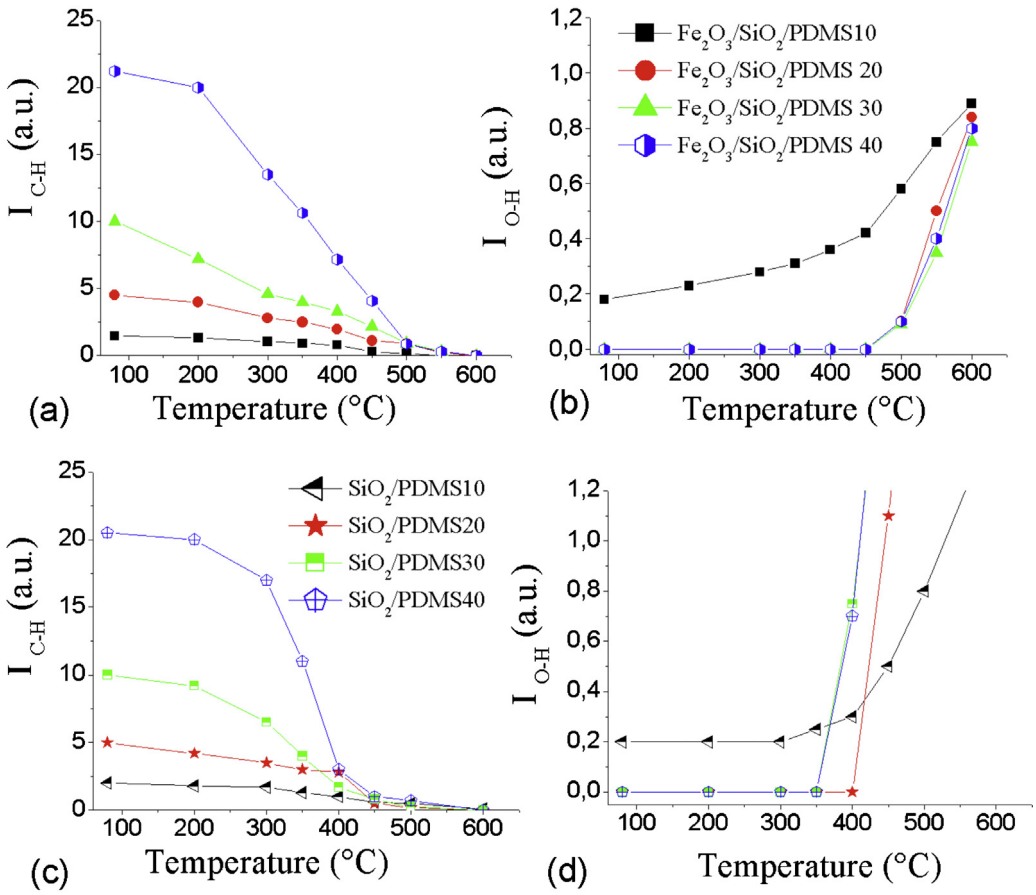

Fig. 4. Integral intensity of CH (a and c) and OH-stretching vibrations (b and d) of CH_3 groups and free silanols, normalized to the intensity of the band at 1865 cm^{-1} for the Fe_2O_3/SiO_2/PDMS (a and b) and SiO_2/PDMS (c and d).

of PDMS decomposition on surface silanols enhances the hydrophobic properties. Further increasing of heating temperature up to 550 °C leads to complete oxidation of the methyl groups and restoring of the surface silanol groups; therefore, the surface becomes more hydrophilic. These results are in good agreement with the FTIR spectroscopy data (Fig. 4).

Thus, Fe_2O_3 nanoparticles in composites with silica and PDMS promote hydrophobic properties of the polymer coating. On the other hand, there is correlation between the reduction of the temperature of PDMS degradation and increasing hydrophobic properties in the presence of Fe_2O_3.

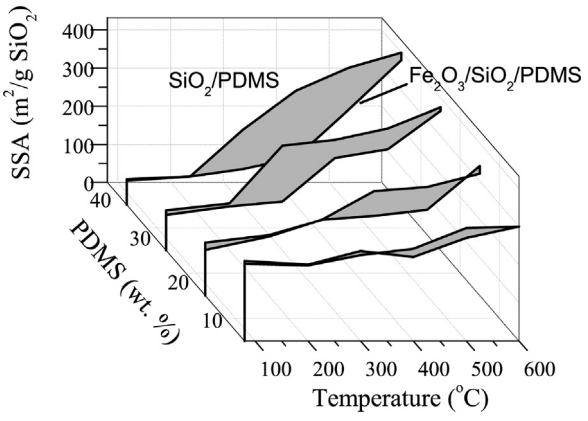

Fig. 5. Specific surface area of PDMS/oxide after calcination at 80–600 °C (the upper lines are SiO_2/PDMS and the bottom lines—Fe_2O_3/SiO_2/PDMS samples).

3.3. DSC measurements

Results obtained by the TSDC, RDS, and DSC techniques indicate the presence of an interfacial PDMS layer around the Fe_2O_3 and silica nanoparticles with the structure/morphology and chain dynamics modified in comparison with the bulk polymer.

DSC measurements of Fe_2O_3/SiO_2/PDMS nanocomposites at different contents of PDMS (Fig. 7) give glass transition temperature T_g determined as a midpoint of the heat capacity step at glass transition [14]. The crystallization (T_c) and melting temperatures (T_m) were determined as the peak temperatures of the corresponding peak. In the cooling scans, the glass transition peak is observed around −130 °C (C_{PDMS} = 30 and 40 wt%), and the single exothermic peak of crystallization is at −97 °C (C_{PDMS} = 40 wt%). Heating scans show changes in the thermal transitions of the polymer in the temperature range from −175 °C to 0 °C with increasing PDMS content. The glass transition temperature tends to increase with increasing amount of polymer (Table 2). Here T_g refers to the fraction of amorphous polymer which is not immobilized. The rise of T_g of the amorphous mobile phase can be interpreted as packing of the polymer chains in voids between nanoparticles in aggregates [7]. At the same time, the glass transition range shows no systematic variation with composition (Fig. 7).

In the case of nanocomposites with a large content of PDMS, an exothermic event is observed close to the T_c region, representing cold crystallization [8]. This is a result of uncompleted crystallization during cooling. For lower PDMS contents and pure PDMS, this phenomenon is absent indicating that at the used cooling rate (10 °C/min) crystallization is completed. Thus, only with increasing polymer content and decreasing oxide nanoparticles content the

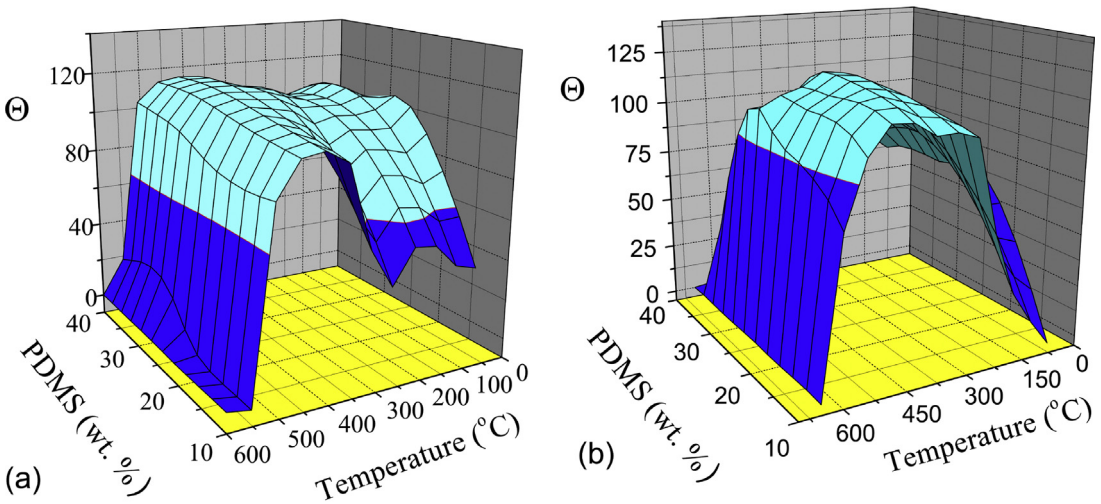

Fig. 6. Dependence of the contact angle of water drops on calcination temperature of (a) Fe_2O_3/SiO_2/PDMS and (b) SiO_2/PDMS.

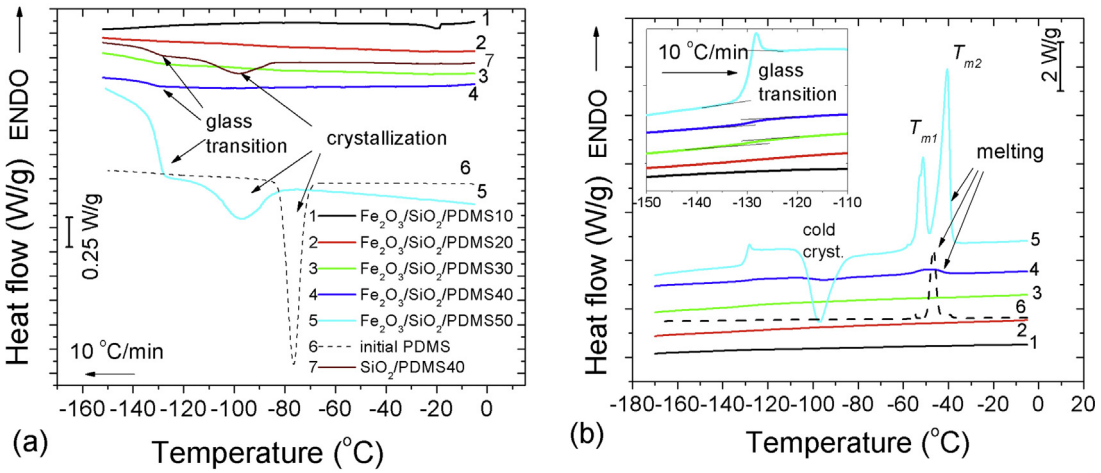

Fig. 7. DSC thermograms of Fe_2O_3/SiO_2/PDMS heated at 80 °C at different polymer contents, during (a) cooling and (b) heating; inset in (b) shows the temperature region of glass transition.

creation of crystallization nuclei is observed. It follows that crystallization in these materials takes place not close to the nanoparticles [15], which also provide constraints for the diffusion of the polymer chains and the growth of the crystals.

At higher temperatures, endothermic melting peaks are observed between −60 °C and −28 °C. Previously, double melting peaks have been observed in the PDMS systems [25]. The secondary weaker melting peak precedes the main one by 10–12 °C.

The crystallinity is observed only at C_{PDMS} = 80 wt%. The nonlinear concentration dependences of the thermodynamic characteristics of the composites can be explained by changes in the relative amounts of polymers being in contact with filler nanoparticles and the corresponding changes in the mobility and density of PDMS in the interfacial layer in comparison with the bulk polymer.

Above 250 °C, the mass loss (Fig. 3d) results from the removal of strongly adsorbed water and from the dehydration of surface hydroxyls. It is known that Fe_2O_3 contains various forms of water and hydroxyl groups. According to [20], the number of hydroxyl groups per nm^2 of iron oxide surface is 4.4–10.0 (hematite), 5.1–9.8 (maghemite), and 5–5.2 (magnetite). Surface hydroxyl groups can be linked to one (FeOH), two (Fe_2OH) or three (Fe_3OH) surface iron atoms. There are geminal (twin) hydroxyls, i.e. two hydroxyls

Table 2
DSC data for Fe_2O_3/SiO_2/PDMS samples at different polymer content heated at 80 °C.

	T_c (°C)	ΔH_c (J/g) (±0.5)	$X_{c,cryst}$ (±5%)	T_g (°C) (±0.5 °C)	$\Delta C_{p,n}$ (J/g K) (±0.02)	ΔH_{cc} (J/g) (±0.5)	T_{m1} (J/g)	T_{m2} (°C)	ΔH_m (J/g) (±0.5)	$X_{c,melt}$ (±0.05)
Fe_2O_3/SiO_2/PDMS10	–	0	0.00	–	0.00	0	–	–	0	0.00
Fe_2O_3/SiO_2/PDMS20	–	0	0.00	–	0.00	0	–	–	0	0.00
Fe_2O_3/SiO_2/PDMS30	–	0	0.00	−129	0.22	0	–	–	0	0.00
Fe_2O_3/SiO_2/PDMS40	–	0	0.00	−129	0.17	3	−49	–	4	0.07
Fe_2O_3/SiO_2/PDMS80	−97	3	0.10	−130	0.44	17	−51	−41	25	0.27
PDMS initial	−78	30	0.8	−124	0.81	30	−48		30	

Note: Thermal (DSC) data determined from (i) cooling scan: crystallization temperature T_c, crystallization enthalpy ΔH_c and degree of crystallinity as calculated from the crystallization peak $X_{c,cryst}$, (ii) heating scan: temperature and normalized heat capacity change of glass transition T_g and $\Delta C_{p,n}$, respectively, cold crystallization enthalpy ΔH_{cc}, melting peak temperatures T_{m1} and T_{m2}, melting enthalpy ΔH_m, and degree of crystallinity calculated from the melting peak $X_{c,melt}$.

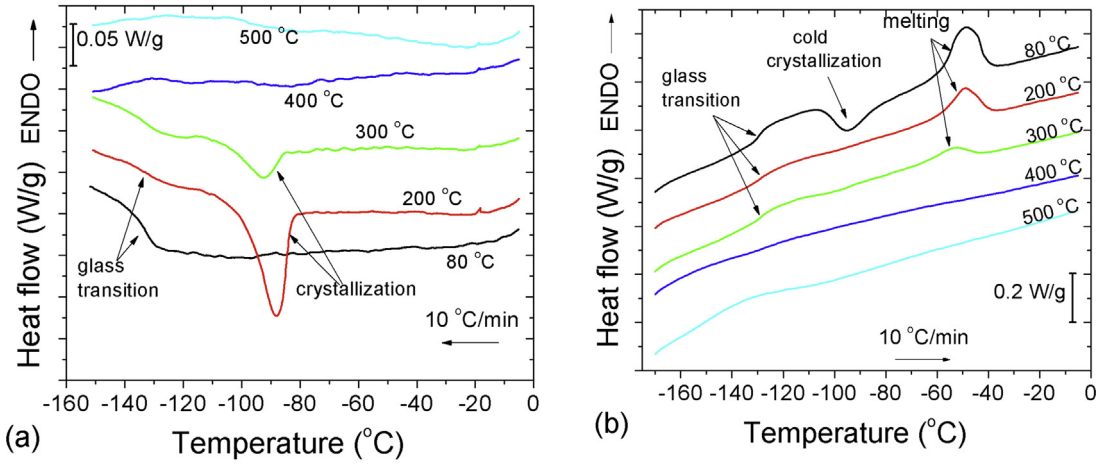

Fig. 8. DSC thermograms of Fe_2O_3/SiO_2/PDMS (40 wt%) heated at various temperatures, during (a) cooling and (b) heating.

bound to the same iron atom. Thus, appearance of the single exothermic peak of crystallization around −97 °C (Fig. 8), after calcination at 200 °C, can be attributed to the removal of physically adsorbed water that contained in the polymer. This water prevents the polymer chains mobility during freezing of the samples. After heating up to 150–200 °C, water evaporates and the chains remain more mobile during subsequent cooling.

3.4. Thermally stimulated depolarization currents (TSDC)

TSDC measurements of α- and α′ relaxations (Fig. 9) give information about the nature of interactions of the polymer with the oxide surface, since α relaxation is the segmental relaxation of free (bulk) polymer chains, associated with the glass transition of the amorphous phase of PDMS, whereas α′ is defined as the segmental relaxation of PDMS chains in the interfacial layer close to the silica surface [8]. Chain mobility in the interfacial layer is constrained due to hydrogen bonding of the oxygens on the polymer backbone to the hydroxyls on the silica surface and dispersion interactions with silica particles [26]. The thermogram of pure PDMS shows a peak at −132 °C, which corresponds to the segmental α relaxation. The temperature T_α of the peak maximum is in good agreement with the DSC data (T_g). of the α′ relaxation, located between −120 °C and −90 °C in the nanocomposites is absent in unfilled PDMS, in agreement with and in support of the assignment of the relaxation to polymer chains in the interfacial layer around the nanoparticles. The results in Fig. 9 show that the overall dielectric response and, in particular, the dielectric strength of both α and α′ relaxations increases with increasing PDMS content.

For the Fe_2O_3/SiO_2/PDMS nanocomposites the peak temperature of α relaxation (between −150 °C and −125 °C) shifts toward higher temperatures with decreasing PDMS content (arrows in Fig. 9b), indicating an overall reduction of molecular mobility of the polymer matrix with increasing filler content, due to constraints imposed by the filler particles [7].

Additionally, a shoulder appears on the high-temperature wing of the main α peak extending up to approximately 30–40 °C higher, with its intensity increasing with increasing PDMS content. Following previous extensive work [5,26], the shoulder, present also in neat PDMS, is assigned to the α_c relaxation of PDMS chains in a layer of amorphous polymer confined between crystal regions. Then, the main relaxation at about −132 °C in the composites is assigned to α relaxation of the PDMS chains in larger amorphous regions that are sufficiently far from the oxides-nanoparticles. The α_c relaxation (at about −123 °C) is faster and stronger than α′ and its position is not affected directly by the nanoparticles. The strength of this relaxation decreases with reduction of crystallinity degree X_c, which is in agreement with its assignment. Finally, the events recorded in

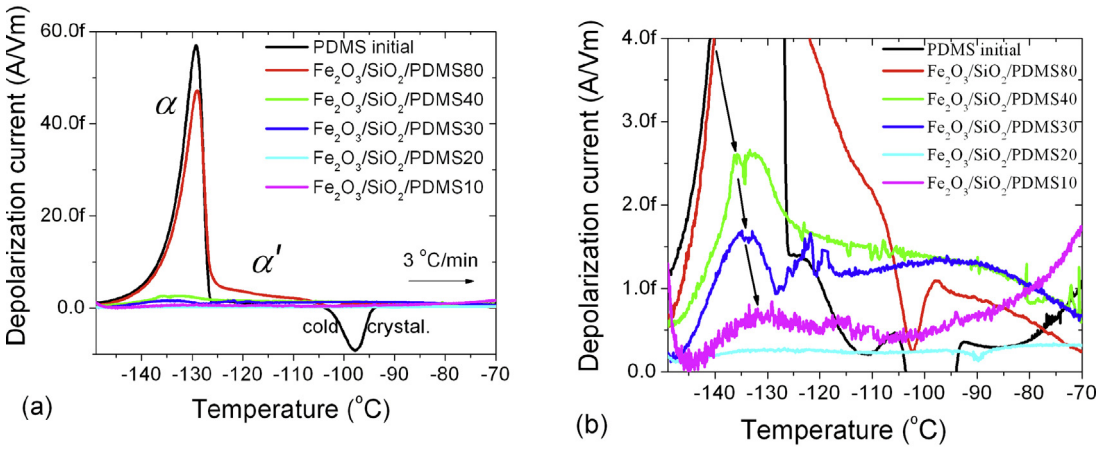

Fig. 9. Comparative TSDC thermograms of PDMS and Fe_2O_3/SiO_2/PDMS at various contents of PDMS. Thermograms are presented in full current range (a) and in more detailed scale for the nanocomposites (b). The arrows in (b) show changes with decreasing polymer content.

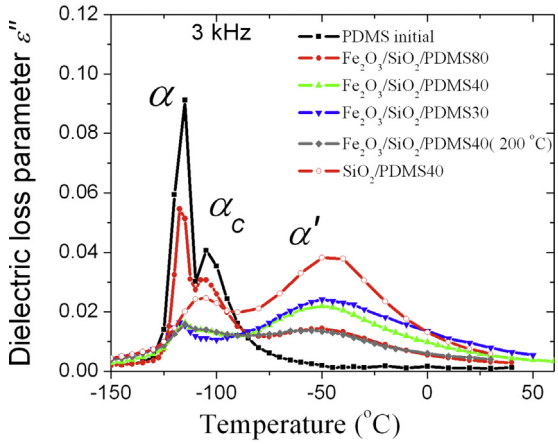

Fig. 10. Comparative isochronal DRS plots of ε'' vs. temperature at 3 kHz for initial PDMS and nanocomposites.

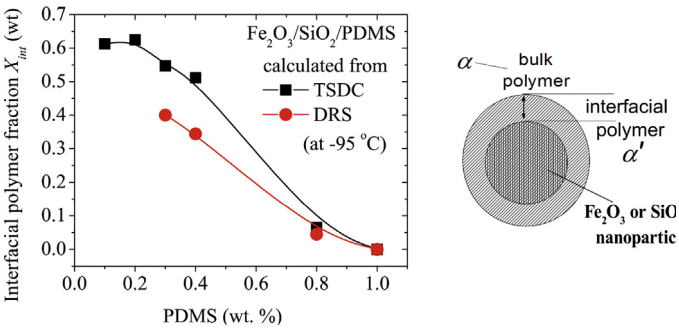

Fig. 12. The fraction of PDMS with reduced mobility vs. polymer content obtained from Eq. (4). The scheme on the right shows the simplified model used to estimate the interfacial and bulk polymer phases.

the temperature range between −105 °C and −94 °C are related to cold crystallization.

3.5. Dielectric relaxation spectroscopy (DRS)

DRS was used to investigate molecular dynamics in the bulk and interfacial layers by following the temperature dependence of the corresponding dielectric relaxations. DRS results are presented here in the form of temperature (Fig. 10, isochronal plot) and frequency dependencies (Fig. 11, isothermal plot) of the imaginary part of dielectric permittivity (dielectric loss) ε''. We focus here on segmental dynamics, i.e. the dielectric relaxations α, α_c and α′ corresponding to the TSDC data in the temperature range between −70 °C and −150 °C (Fig. 9b). A higher frequency of 3 kHz was selected for (Fig. 10), as compared to TSDC (Fig. 9) to suppress conductivity effects [16].

Several relaxations can be observed in the isocronal plots of Fig. 10, the same as with TSDC (Fig. 9: α, α_c, and α′, in the order of increasing temperature, with the assignment described above. Included in Fig. 11(a) are also results obtained with initial silica, where the response is dominated by a strong relaxation (*S* relaxation), arising from motion of hydroxyls on the silica surface, in agreement with previous results [5,8,10,11]. All these relaxations are thermally activated, shifting toward higher frequency with increasing temperature in the isothermal plots or to higher temperature with increasing frequency in the isochronal plots. Comparing the isochronal plots in Figs. 9 and 10 to each other, a shift of the relaxations to higher temperatures is observed in Fig. 10, obviously due to the higher frequency of presentation [26].

It can be seen that in the case of SiO_2/PDMS40, only α″ and α_c relaxations are present. So all PDMS (40 wt%) interacts with the silica surface (α′) or crystallizes (α_c). In the case of Fe_2O_3/SiO_2/PDMS, α relaxation increases with increasing PDMS content, while α′ relaxation decreases indicating, that the main part of PDMS is in amorphous phase and only a small part can interact with the oxide surface. The α_c relaxation can be observed only in samples with 40–80 wt% of PDMS. The results are in good agreement with the TSDC data.

The α, α′, α_c relaxations are observed for Fe_2O_3/SiO_2/PDMS also in the isothermal plots of Fig. 11, where their shift to higher frequency with increasing temperature can be also observed. It is interesting to note with respect to the *S* relaxation, arising from motion of hydroxyls on the silica surface, as mentioned above, that this relaxation practically disappears in the nanocomposites, even at high filler contents, indicating that the hydroxyls are now encaged in hydrogen bonding interactions with PDMS. Of particular interest is also that, based on the values of the crystallinity degree calculated from DSC data (Table 2) and the strength and frequency range of the α_c relaxation, we can confirm that this relaxation is similar to that observed in the TSDC thermograms.

The combined use of DSC, TSDC, and DRS provided clear evidence on the origins of the relaxations described above. Thus, we can use now the data for the dielectric strength from TSDC

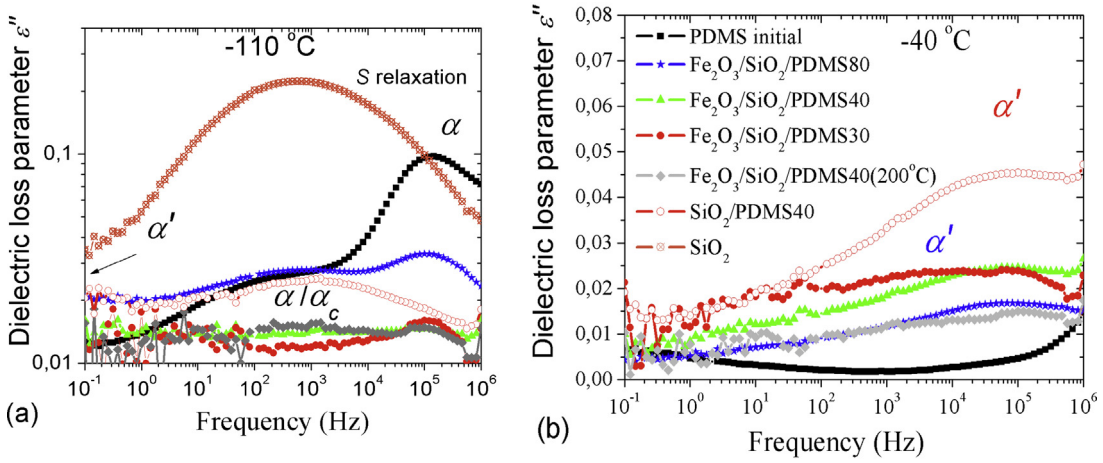

Fig. 11. Comparative isothermal DRS plots of ε'' vs. frequency for initial PDMS and nanocomposites at −110 °C (a) and −40 °C (b).

Table 3
Characteristics of the polymer in SiO_2/PDMS and Fe_2O_3/SiO_2/PDMS (40 wt%) heated at 80 °C.

Sample	T_{treat} (°C)	T_c (°C)	ΔH_c (J/g) (±0.5)	$X_{c,cryst}$ (±0.05)	T_g (°C) (±0.5)	$\Delta C_{p,n}$ (J/g K) (±0.02)	ΔH_{cc} (J/g) (±0.5)	T_{m1} (J/g)	T_{m2} (°C)	ΔH_m (J/g) (±0.5)	$X_{c,melt}$ (±0.05)
SiO_2/PDMS40	80	−99	3	0.20	−129	0.25	5	−49	−44	9	0.27
	300	–	0	0.00	–	0.00	0	–	–	0	0.00
	500	–	0	0.00	–	0.00	0	–	–	0	0.00
Fe_2O_3/SiO_2/PDMS40	80	–	0	0.00	−129	0.17	3	−49	–	4	0.07
	200	−88	3	0.20	−128	0.14	0	−49	–	3	0.20
	300	−92	1	0.07	−128	0.11	0	−54	–	1	0.07
	400	–	0	0.00	–	0.00	0	–	–	0	0.00
	500	–	0	0.00	–	0.00	0	–	–	0	0.00

or DRS measurements, combined with the data for the degree of crystallinity, obtained from DSC measurements, to calculate the reduced mobility polymer fraction X_{int} (the fraction of polymer in the interfacial layer, Fig. 12) by the following equation

$$X_{int} = \frac{\Delta\varepsilon_{\alpha'}(1 - X_c)}{\Delta\varepsilon_{\alpha'} + \Delta\varepsilon_{\alpha}}, \quad (4)$$

where $\Delta\varepsilon$ is the dielectric strength of each relaxation [8,26] and X_c is the crystallinity degree of each sample (Table 3). Calculations were carried out using both TSDC and DRS data and the results are presented in Fig. 12.

4. Conclusion

Nanoparticles of iron oxides in the Fe_2O_3/SiO_2/PDMS systems catalyze the thermal decomposition of PDMS and increase the contribution of depolymerization processes. Hydrophobicity of Fe_2O_3/SiO_2/PDMS heated at 100–650 °C is higher than that of SiO_2/PDMS treated at the same temperatures. Molecular dynamics in the nanocomposites were studied using DSC and dielectric (TSDC, DRS) techniques. Three discrete relaxations in the region of the glass transition of PDMS were identified and studied, arising from the segmental mobility of the bulk (unaffected) polymer (α relaxation), the mobility of polymer chains restricted between condensed crystalline regions (α_c relaxation), and the segmental dynamics in the interfacial polymer layer around the oxide nanoparticles (α′ relaxation).

Acknowledgments

The research leading to these results has received partial support from the European Community's Seventh Framework Programme (FP7 2007–2013, grant 230790, Compositum). This research has been co-financed by the European Union (European Social Fund–ESF) and Greek National Funds through the Operational Program "Education and Lifelong Learningöf the National Strategic Reference Framework (NSRF)—Research Funding Program: Heracleitus II. Investing in knowledge society through the European Social Fund (P.K and P.P.), and Research Funding Program: Aristeia (P.P.).

References

[1] N. Yamada, I. Yoshinaga, S. Katayama, J. Sol-Gel Sci. Technol. 17 (2000) 123–130.
[2] A. Akinci, Arch. Mater. Sci. Eng. 35 (2009) 29–32.
[3] X.X. Wang, H.T. Wang, X.M. Song, G.Q. Wang, Q.G. Du, Q.T. Chen, Express Polym. Lett. 4 (2010) 373–381.
[4] J.A. Wen, J.E. Mark, J. Appl. Polym. Sci. 58 (1995) 1135–1145.
[5] P. Klonos, A. Panagopoulou, A. Kyritsis, L. Bokobza, P. Pissis, J. Non-Cryst. Solids 357 (2011) 610–614.
[6] K.S. Chen Yang, J. Appl. Polym. Sci. 86 (2002) 414–421.
[7] V. Bershtein, L. Egorova, P. Yakushev, P. Pissis, P. Sysel, L. Brozova, J. Polym. Sci., Part B: Polym. Phys. 40 (2002) 1056–1069.
[8] P. Klonos, A. Panagopoulou, L. Bokobza, A. Kyritsis, V. Peoglos, P. Pissis, Polymer 51 (2010) 5490–5499.
[9] D. Fragiadakis, P. Pissis, L. Bokobza, Polymer 46 (2005) 6001–6008.
[10] R.H. Gee, R.S. Maxwell, G.B. Balazs, Polymer 45 (2004) 3885.
[11] G. Tsagaropoulos, A. Eisenberg, Macromolecules 28 (1995) 6067.
[12] V. Arrighi, I. McEwen, H. Qian, M. Prieto, Polymer 44 (2003) 6259.
[13] V. Arrighi, J. Higgins, A. Burgess, G. Floudas, Polymer 39 (1998) 6369.
[14] M. Sorai, Comprehensive Handbook of Calorimetry and Thermal Analysis, Wiley, West Sussex, 2004.
[15] M. Aranguren, Polymer 39 (1998) 4897–4990.
[16] P. Bräunlich, Thermally Stimulated Relaxation in Solids, Springer, Berlin Heidelberg, 1979.
[17] F. Kremer, A. Schoenhals, Broadband Dielectric Spectroscopy, Springer, Berlin, 2003.
[18] G.L. Mack, D.A. Angles, The Determination of Contact Angles from Measurements of the Dimensions of Small Bubbles and Drops, New York, NY, 1935.
[19] G. Voronkov, V.P. Meleshkevich, Y.A. Yuzhelevsky, Siloxane Bond, Novosibirsk, Nauka, 1976.

[20] R.M. Cornell, U. Schwertmann, The Iron Oxides: Structure, Properties, Reactions, Occurrences and Uses, second ed., Wiley-VCH, Weinheim, 2003.
[21] T.I. Denisova, J. Therm. Anal. Calorim. 62 (2000) 523–527.
[22] G. Gamino, S.M. Lomakin, M. Lageard, Polymer 43 (2002) 2011–2015.
[23] V.M. Bogatyrov, M.V. Borysenko, J. Therm. Anal. Calorim. 62 (2000) 335–344.
[24] N.P. Kharitonov, V.V. Ostrovsky, Thermal and Thermooxidizing Destruction of Polyorganosiloxanes, Nauka, Leningrad, 1982.
[25] M. Soutzidou, A. Panas, K.J. Viras, J. Polym. Sci. Pol. Phys. 36 (1998) 2805–2810.
[26] D. Fragiadakis, P. Pissis, J. Non-Cryst. Solids 353 (2007) 4344–4352.